Words: 3,790
Tables: 7
Figures: 1

Functional Neuroimaging Distinguishes Autism Spectrum Disorder from Healthy and Comorbid Conditions in Focused and Large Community Datasets

Daniel G. Amen, MD, PhD[1]
Kristen Willeumier, PhD[1]
Derek Taylor[1]
Sandlin Lowe, MD[1]
Cyrus Raji, MD, PhD[2]

Corresponding Author:
Daniel G. Amen, M.D.
Amen Clinics, Inc.
3150 Bristol Street, Suite 400
Costa Mesa, CA 92626
T: (949) 887-8315 F: (949) 266-3780
docamen@amenclinics.com
www.amenclinics.com

Key Words: neuroimaging, autism spectrum disorder (ASD), Single Photon Emission Computed Tomography (SPECT), biomarker

Abstract

Background: The diagnosis of Autism Spectrum Disorder (ASD) relies on history and observation, as no reliable biomarkers have been published. Here we performed a retrospective data mining analysis of 933 ASD patients to investigate whether reliable biomarkers exist for distinguishing ASD from healthy controls in adults, as well as between ASD and non-ASD patient cohorts of adults and children.

Methods: Subjects were obtained from a multisite psychiatric database which included rest and on task brain SPECT scans. Data analysis was performed across eleven cohorts including healthy adult controls, adult and child patients with ASD, mood disorders, anxiety disorders, attention deficit hyperactivity disorders (ADHD), and non-ASD matched controls. Scan regions of interest (ROIs) and visual readings were analyzed using a binary logistic regression model with predicted probabilities inputted into a receiver operating characteristic analysis to identify sensitivity, specificity, and accuracy. Forward stepwise logistic regression was used to identify the most diagnostically significant regions.

Results: Rest and on-task ROIs and visual readings significantly differentiate ASD adults from healthy controls as well as ASD adults and children from mood disorders, anxiety disorders, ADHD and non-ASD matched controls. Decreases in blood flow were observed in the prefrontal cortex, thalamus, parietal and temporal lobes, cerebellum, cerebellar vermis, amygdala, angular gyrus and rolandic operculum in those with ASD. In select groups, increases were noted in the prefrontal pole, and temporal and superior parietal lobes.

Conclusions: Using this method, our findings suggest that SPECT is able to reliably distinguish ASD patients from healthy controls in adults and ASD patients from mood disorders, anxiety disorders, ADHD and non-ASD matched controls in children and adults. These findings may

provide useful diagnostic biomarkers to identify ASD from healthy and comorbid psychiatric disorders.

Background

According to the Diagnostic and Statistical Manual of Mental Disorders, 5th Edition (DSM-V), autism spectrum disorder (ASD) is a group of neurodevelopmental syndromes defined by problems which manifest early in childhood in three domains: social interactions, communication, and restricted, repetitive patterns of interests or behaviors [1]. In the previous version of the DSM [2], ASD was categorized under Pervasive Developmental Disorders (PDD), which included Autism, Asperger's Syndrome, Childhood Disintegrative Disorder, and Pervasive Developmental Disorder not otherwise specified (PDD-NOS). As research put the validity of the categorical distinctions in doubt, DSM-V classified all these diagnoses together under the ASD umbrella.

This broader categorization fits with the widely held belief that ASD is not a unitary disorder, but rather has multiple types and etiologies [3], including genetic [4-6], epigenetic [7], inflammatory [8,9], toxic [10] and infectious [11,12]. Comorbidity is high in ASD with 70% having at least one comorbid condition and 41% having two or more [13]. The most common diagnoses were social anxiety disorder (29.2%), attention-deficit/hyperactivity disorder (28.2%), and oppositional defiant disorder (28.1%). There are also a group of clinical issues that commonly occur in ASD, such as seizure disorders, immune dysregulation, sleep disturbances, and gastro-intestinal dysfunction [14].

For reasons not well understood, ASD is increasing in prevalence and, at the time of this writing, is reported to affect 1 in 68 individuals and is five times more likely in males than females [15]. Early intervention has been associated with positive outcome results [16-18].

The assessment of ASD typically involves clinical history, physical examination, and structured screening tools [19]. Functional neuroimaging is not part of routine evaluations

because no reliable biomarkers have been found or published. Finding reliable, sensitive, and specific neuroimaging biomarkers could help in the diagnostic process and also help understand the underlying physiological individual variability in patients.

Brief Literature Review on Imaging and ASD

Multiple functional and structural neuroimaging techniques have shown ASD abnormalities, most notably in the cerebellar vermis, anterior cingulate gyrus, amygdala, hippocampus, and areas of the frontal, temporal and parietal lobes. The most consistent structural and volumetric findings for ASD are accelerated brain volume growth in early childhood in both white and gray matter [20]. Connectivity problems have been seen between brain regions [21-24].

A recent meta-analysis by Stanfield et al. [25] of 43 structural neuroimaging studies of over 800 ASD subjects between 3 and 30 years of age found larger total brain volume and basal ganglia in ASD with decreased volumes in other regions, especially the cerebellar vermis, as compared to controls. Cerebellar abnormalities are the most commonly reported finding in autism, and have been present in the literature since 1988 when Courchesne et al. [26] first reported decreased volumes of vermian lobules VI and VII in patients with autism. These findings were confirmed by Stanfield et al. [25]. Increased volume in the basal ganglia has been correlated to repetitive behaviors observed in autism [27,28]. Investigations of structural measures of the cingulate have reported decreased size associated with decreased metabolic activity in ASD [29]. Volumetric abnormalities have also been reported, particularly in the frontal lobes [30] in addition to the temporal [31,32] and parietal lobes [33]. A meta-analysis of voxel-based morphometry (VBM) [34] on 496 ASD subjects found smaller gray matter volume

in the ASD group compared to controls in the amygdala-hippocampus complex and medial parietal regions.

Philip and colleagues [35] reviewed 90 fMRI studies in ASD across multiple functional domains and found decreased prefrontal activation during executive function tasks and decreased activation in the temporal lobes during tasks related to auditory and language processing. Since 1992, there have been over 55 studies using brain single photon emission computed tomography (SPECT) and positron emission tomography (PET) imaging in over 900 ASD patients. The findings have primarily shown lower perfusion in the prefrontal cortex, temporal lobes, parietal lobes and cerebellum compared to controls [36-41]. However, most of the studies were small, and none of the studies looked at the potential sensitivity and specificity of using SPECT or PET as a diagnostic tool to distinguish between healthy and non-ASD patient controls. Here, we performed a retrospective data mining analysis of a comprehensive brain SPECT imaging database to evaluate whether SPECT has the power to differentiate ASD from healthy controls and non-ASD patient controls with adequate sensitivity and specificity.

Methods:

Study Subjects:

This study was conducted in accordance with the STARD guidelines (http://www.stard-statement.org/). All subjects were obtained from a large, multisite, clinical psychiatric database involving 27,756 patients collected from 1995-2014. The patients came for evaluation of complex, treatment resistant psychiatric issues to one of nine outpatient clinics (Newport Beach, Costa Mesa, Fairfield, and Brisbane, CA; Tacoma and Bellevue, WA; Reston, VA; Atlanta, GA; and New York, NY) and had rest and on-task SPECT scans as part of their evaluation.

Diagnoses were made by board certified or board eligible psychiatrists using all of the data available to them, including a detailed clinical history, mental status examination, and DSM-IV or DSM-V criteria. Informed consent was obtained from all patients or legal guardians to allow their anonymous clinical data to be utilized for research purposes. This retrospective review was approved by IntegReview (www.integreview.com), an independent institutional review board (IRB #004).

Included in the database are 99 healthy adult volunteers who each had rest and on-task SPECT studies. The exclusion criteria for the healthy subjects were the following: 1) current or past evidence of psychiatric illnesses as determined by a detailed clinical history, mental status examinations, and the Structured Clinical Interview for Diagnosis for DSM-IV (SCID-IV); 2) current reported medical illnesses or medication; 3) history of brain trauma; 4) current or past drug and alcohol abuse; and 5) family history of a first degree relative with a psychiatric illness. Written informed consent was obtained from all healthy subjects under an approved IRB protocol (WIRB # 20021714).

Five groups were extracted from the larger database for analysis and are detailed in Table 1. These include: 1) healthy controls; 2) adults with ASD; 3) adults without ASD matched for age, gender, and diagnoses; 4) children (<18 years of age) with ASD; and 5) children without ASD matched for age, gender, and diagnoses. Six subgroups were also extracted from the non-ASD matched controls, including 1) adults with mood disorders (major depression, dysthymia, bipolar disorder, cyclothymia, and depression NOS); 2) adults with anxiety disorders (generalized anxiety disorder, panic disorder, posttraumatic stress disorder, simple and social phobias, and obsessive compulsive disorder); 3) adults with ADHD (combined type, primarily inattentive type, and primarily hyperactive-impulsive type); 4) children with mood disorders; 5)

children with anxiety disorders (overanxious disorder plus those listed above); and 6) children with ADHD.

SPECT Imaging:

SPECT was obtained in conjunction with clinical assessments before any intervening treatment. Brain SPECT was applied as previously described in published work using standard methods [42,43]. To review, in each study, an age- and weight-appropriate dose of technetium Tc99m exametazime (commercially available as Ceretec™) was administered intravenously. Rest scans were performed in the following manner. Patients sat upright with eyes open in a quiet, dimly lit room where IV access was obtained. Ten minutes later, the radiopharmaceutical was injected. Patients sat for an additional ten minutes post-injection and were scanned approximately 30 minutes after injection. On-task scans were performed in the following manner. Patients sat upright with eyes open in a quiet, dimly lit room where IV access was obtained. Then they started a 15-minute computerized concentration task, the Conners Continuous Performance Test II (CCPT-II, Multi-Health Systems, Toronto, Ontario). The radiopharmaceutical was injected three minutes after starting the 15-minute test. Approximately 30 minutes after the injection, subjects were scanned. Photon emission was captured using a high resolution Picker Prism XP 3000 triple-headed gamma camera (Picker Int. Inc., Ohio Nuclear Medicine Division, Bedford Hills, OH, USA) with low energy high resolution fan beam collimators. Data was acquired in in 128x128 matrices, yielding 120 images per scan with each image separated by three degrees spanning 360 degrees. Chang attenuation correction was performed using linear methods and a linear attenuation coefficient of 0.151 [44]. Transaxial

slices oriented horizontal to the AC-PC line were created along with coronal and sagittal images (6.6mm apart, unsmoothed).

SPECT Region of Interest Analysis:

These quantitative ROI metrics were not used to aid in the clinical diagnosis. The processed reconstructed images were spatially normalized and realigned using a mutual information based affine registration [45] algorithm implemented using the ITK Insight Toolkit [46]. Mutual information registration algorithm used in ROI Extract finds an affine transformation of a canonical SPECT scan template in MNI space that minimizes the joint entropy between the unchanged individual image and the transformed atlas image. The resulting affine transformation matrix is then applied to the atlas label map, transforming it into the subject specific space. Once the atlas has been transformed into the individual space, ROI metrics can be calculated. The Automated Anatomical Labeling (AAL) atlas was used for ROI analysis. [47] The AAL atlas consists of 128 brain regions defined across both hemispheres. ROI metrics included region mean, standard deviation, minimum, maximum, 5^{th} percentile histograms, largest maximum valued connected cluster after thresholding, and largest minimal valued connected cluster after thresholding. These metrics serve to characterize each ROI in terms of maximum and minimum activations within those regions along with providing information on the size of those maxima and minima and histograms of the value distributions within regions. Each of these metrics is potentially useful in discriminating between disease states in the brain when compared to healthy subjects. Each metric is computed and archived in an in-house data management system. To account for outliers, T-score derived ROI count measurements were derived using trimmed means [48] that are calculated using all scores within the 98% confidence

interval (-2.58 < Z < -2.58). The ROI mean for each subject and the trimmed mean for the sample are used to calculate T with the following formula: T = 10*((subject ROI_mean – trimmed regional_avg)/trimmed regional_stdev) +50.

SPECT Visual Reading (VR) Analysis:

In addition, all scans were read visually by experienced SPECT scan readers. Methods for visual readings have already been fully described in prior peer reviewed work [42,43]. To review, 14 gross general cortical regions of interest (ROIs) in orthogonal planes were visually inspected and rated using the Mai Atlas of the Human Brain [49]: the left and right prefrontal poles (medial aspect of Brodmann area [BA] 10, anterior rostral aspect of BA 12); the left and right inferior orbits (BA 11); the left and right anterior/lateral PFC (comprised of BAs 45, 46, 47, the anterior aspect of area 9, and the lateral aspect of area 10); the left and right midlateral PFC (BAs 8 and 44, and the posterior aspect of area 9); the left and right posterior frontal region (BAs 4, 6, and the anterior aspect of area 43); the left and right parietal lobes (BAs 1, 2, 3, 5, 7, 39, and 40, and the posterior aspect of area 43); and the left and right occipital lobes (BAs 17, 18, and 19). In like manner, we rated the left and right cerebella. In addition, seven gross subcortical ROIs were rated: the anterior cingulate gyrus (BAs 25, 32, 33, and the anterior aspect of BA 24); the left and right insula; the left and right caudate nuclei; and the left and right putamen. Raters did not have access to detailed clinical information, but did know age, gender, medications, and primary presenting problem. The following nonlinear scheme was used to visually rate rCBF: activity rated above the top 95% was assigned a score of 4+; 91%-95% was scored 3+; 86%-90% was scored 2+; 81%-85% was scored 1+; 61%-80% was scored 0; 56%-60% was scored –1; 51%-55% was scored –2; 46%-50% was scored –3; and 41%-45% was

scored –4. Each area was rated for its highest and lowest activity, and the average of the two was taken as a given ROI's final rating, resulting in a rating scale ranging from +4 to -4 in ½-point intervals.

Statistical Analyses:

All analyses were performed using Statistical Package for Social Science (SPSS, version 22, IBM, Armonk, NY). Data were analyzed first at Amen Clinics (D.A.) with analyses repeated and results verified independently at UCLA (C.R.). Multiple imputation analysis did not identify any significant missing data (<10%) in this analysis.

Data were analyzed in the following steps: First, binary logistic regression models were built using either rest ROIs, rest visual reads, on-task ROI, or on-task visual reads as predictor variables. Paired comparisons between the different groups were achieved. Covariates in the analysis were age, gender, race, and psychiatric co-morbidities listed in Table 1. Predicted probabilities from binary logistic regression models were then inputted into a receiver operating characteristic (ROC) analysis to identify sensitivity, specificity, and accuracy in delineating between the various clinical groups with 95% confidence intervals. Finally, forward stepwise logistic regression was invoked in SPSS to identify the most diagnostically significant regions in comparing ASD to the groups listed and then a One Way ANOVA with Least Square Differences (LSD) for correcting for multiple comparisons were done to confirm statistically significant difference ($p < .05$) and to determine if increases or decreases in these diagnostically important regions were the main predictors of diagnostic utility of the SPECT regions tested.

Results:

Using ROI analysis both at rest and on-task, ASD patients showed significant separation from the healthy adult cohort with 100% accuracy, 100% sensitivity and 100% specificity at rest and on-task, while the visual readings (VR) revealed a separation between 90-98% across all measures, respectively. Furthermore, the ROI analysis in adults separated mood disorders, anxiety disorders and ADHD from ASD with 100% accuracy. With the matched comorbidity, accuracy was 84% at rest and 86% on-task. VR analysis in adults revealed that the separation was less robust but still significant ($p<0.01$) with accuracy between 79-92%. With the matched comorbidity, accuracy with VR was 73% at rest and 77% on-task. See Table 2 for results.

The ROI analysis in children separated mood disorders, anxiety disorders, and ADHD from ASD with accuracy between 91-100% at rest and 90-100% on task. With the matched comorbidity, accuracy was 79% at rest and 81% on-task. For the VR child groups, the separation was less robust but still significant ($p<0.01$) with accuracy between 70-93% for rest and 77-84% for on-task. With the matched comorbidity, accuracy with VR was 70% at rest and 66% on-task. See Table 3 for results.

For regional differences separating ASD from healthy controls, commonly co-morbid psychiatric disorders and non-ASD matched controls at rest and on-task, refer to tables 4 - 5 for the adult data and tables 6 - 7 for the child data. When comparing adults with ASD across all four psychiatric cohorts, perfusion decreases were most frequently observed in the prefrontal cortex, thalamus, inferior temporal lobes, cerebellar cortices (Crus I, III, VIII, X) and vermis VII. No increased perfusion was observed in ASD during rest or on-task ROI analysis. See tables 4b and 5b for regional increases observed with VR. When comparing children with ASD across all four psychiatric cohorts using ROI analysis, decreased perfusion was most frequently observed in the frontal lobes, amygdala, angular gyrus, rolandic operculum, inferior and superior temporal

lobes, parietal lobes, cerebellar cortices (Crus I, III, IV, V, VI, VII B, IX, X) and vermis (I, II, III, VII, VIII) using ROI analysis. No consistent increases were observed across groups. See table 6 and 7 for regional increases observed in ASD within each group. Using VR, decreases were observed in the medial prefrontal cortex and temporal lobes while increases were observed in the right anterolateral prefrontal cortex in two of the cohorts.

Discussion:

When differentiating ASD from healthy controls, ADHD, mood and anxiety disorders and non-ASD matched controls, ASD showed a significant number of regional perfusion decreases observed using both ROI and VR in brain regions correlated with ASD symptomology. One of the most notable neuropathological hallmarks of ASD includes structural and functional deficits reported in the cerebellar vermis and cortices. Here we observed perfusion deficits across various regions of the cerebellar cortex and vermis in both children and adults which were unique to the comparative diagnostic group. This finding is consistent with the cerebellar atrophy observed with MRI and the correlated behavioral dysfunctions including challenges with coordinated movement, motor sequencing, affective expression and exploratory attention [50]. In children, decreases were observed in ASD across several of the comparative groups with ROI analysis at rest and on-task in the angular gyrus, a region located near the temporal parietal junction (TPJ). Previous research has demonstrated that the right TPJ is a mentalizing region of the brain that responds atypically in those with autism spectrum conditions compared to controls as measured by fMRI [51]. This region has been implicated in the understanding of other's mental states or "theory of mind," [52] language, spatial cognition and attention and may explain the social-communication deficits observed in ASD. Furthermore, we observed reductions in

blood flow in the amygdala, frontal and temporal lobes in ASD children, neural regions that comprise the social brain and are fundamental to social intelligence which have been shown to be hypoperfused in autistics using fMRI [53]. The small number of increases that were observed in children are particularly interesting, especially in the pre and postcentral gyrus, parietal and temporal lobes.

Both the children and adult ASD cohorts showed decreases in regional cerebral blood flow in one or more of the regions consistently described in the ASD imaging literature including the prefrontal cortex, thalamus, parietal lobes, temporal lobes, cerebellar cortices and vermis. [38,40,54-57] These areas of hypoperfusion correlate with the abnormal behavior patterns observed in ASD including issues with attentional dysfunction and modulating social behaviors (frontal lobes), language and emotional processing (thalamus), sensory processing difficulties (parietal lobes), speech and language development (left temporal lobe) social difficulties (right temporal lobe) and movement or motor sequencing (cerebellum). In adults, all ROI analyses revealed decreases in perfusion in ASD as compared to various co-morbid disorders (mood disorders, anxiety and ADHD) and healthy controls, while VR revealed increases in the prefrontal pole, temporal lobe and thalamo-limbic regions. A majority of these increases were observed on-task, which may result from the requisite hyperconnectivity required for focus and sustained attention.

Clinically, the experienced readers in this study identified a specific 3D SPECT imaging pattern often seen with ASD, where the cerebellum resembles the shape of an hourglass or “free weight” which is visualized as narrow in the medial portion (vermis) and fuller on either side. (See Image 1) In the authors’ experience, the “classic” ASD pattern is typically observed as low cerebellar perfusion and increased anterior cingulate and medial prefrontal perfusion.

Additionally, there are many ASD patients who do not have this "classic" pattern, but instead reveals a "toxic" pattern on SPECT seen as an overall decreased perfusion. The rationale for this may be due to the elevated exposure to neurotoxins implicated in neurodevelopmental disabilities like ASD including methyl mercury, ethyl alcohol and lead. [58]

In the adult population there was high degree of separation between ASD patients and healthy controls, as there was between children and adults with ASD and those with mood disorders, anxiety disorders and ADHD. When compared to a larger population with a high comorbidity with other psychiatric disorders, ASD could be distinguished from non-ASD with reasonable ROC which was similar across rest and on-task states with both quantitative and visual analysis. Since ROIs were not used in any way to initially establish the clinical diagnoses, they serve as a particularly rigorous independent predictor of diagnostic category. However, since nuclear medicine physicians and radiologists typically use visual assessment for interpreting scans in a clinical setting, the highly significant results observed with the VR demonstrate the potential clinical utility of SPECT in the differentiation of these neuropsychiatric disorders.

The strengths of this study include scan data acquired both at rest and on-task from a well-validated and widely available functional imaging modality, detailed quantitative analysis, and an extensively chacterized psychiatric population of both children and adults across multiple sites. The large sample size, while a critical attribute, is further enhanced by the separate analysis of carefully matched smaller cohorts. Several potential limitations of the study design must be addressed. First, this was a retrospective study and we acknowledge that higher levels of evidence can be derived from either prospective studies or randomized clinical trials. However, the large sample size and diverse multi-site study optimizes the generalizabilty of the results.

Second, this data set did not have accompanying structural imaging data. Inclusion of this information would have been useful in characterizing any atrophy associated hypoperfusion, particularly in the cerebellum. With that said, in a retrospective review assessing functional and structural abnormalities in young children with ASD using SPECT and MRI, SPECT revealed extensive focal perfusion deficits in the cerebellum, thalamus, parietal and temporal lobes while the MRI was normal [59] which supports the use of functional neuroimaging as a modality to detect pathophysiology of ASD that may not be apparent on quantitative structural neuroimaging. Third, we did not match for IQ as this was a retrospective analysis; therefore, this data must be interpreted across a broad range of intelligence and communication ability. Fourth, our study population was comprised of 19% females. Future prospective studies with a sex-balanced sample of male and female participants matched for IQ is required to validate these findings. And finally, while the diagnosis of ASD was given based on DSM-IV classification by the treating psychiatrist, inclusion of the Autism Diagnostic Interview would be prudent for future work in keeping in alignment with classification utilized in the research literature in addition to adequately assessing the level of functionality of the patients.

Conclusions:

This is the first study using brain SPECT imaging to demonstrate cerebral perfusion differences in a robust sample of ASD subjects compared to healthy controls and a matched co-morbid group across psychiatric conditions (ADHD, anxiety, and mood disorders) in both children and adults at rest and on-task. Our results provide strong support for biomarkers that differentiate these populations with a high sensitivity, specificity and accuracy and indicate key neural areas that have been previously described in the literature that are consistent with deficits

in theory of mind and social intelligence. Differences were observed between ROI results as compared to those obtained from VR, indicating the need for continued investigation and proper interpretation of the results. ROI information is routinely used in research studies while VR are utilized in the clinical setting, so future research is needed to further characterize and interpret these observed differences. Given the heterogeneity of ASD, neuroimaging may offer key insights to aid in the diagnosis and appropriate course of treatment. Our results suggest that brain SPECT imaging in conjunction with highly trained readers, could provide valuable information in differentiating ASD from commonly occurring co-morbid psychiatric disorders in clinical practice.

List of abbreviations:

Ant = Anterior, ADHD = Attention Deficit Hyperactivity Disorder, AAL = Automated Anatomical Labeling, ASD = Autism Spectrum Disorder, DSM-V = Diagnostic and Statistical Manual of Mental Disorders, Genu = Subgenual, HC = Healthy Control, Inf = Inferior, Lat = Lateral, LSD = Least Square Differences, Med = Medial, Mid = Middle, Orb = Orbital, Oper = Operculum, PDD-NOS = Pervasive Developmental Disorder not otherwise specified, PET = Positron Emission Tomography, Post = Posterior, ROC = Receiver Operating Characteristic, ROI = Region of Interest, SPECT = Single Photon Emission Computed Tomography, Sup = Superior, Suppl = Supplemental, Triang = Triangularis, Vent = Ventral, VR = Visual Reading

Competing Interests:

Authors' Conflict of Interest or Financial Disclosure Statements: No author reports a conflict of interest or financial disclosure.

Author's Contributions:

D.A. designed the study and K.W. managed the project. C.R. conducted the statistical analysis with the help of D.A. and D.T. D.A., K.W., S.L. and C.R. wrote the manuscript. All authors discussed the results and implications and commented on the manuscript at all stages.

Author's Information:

Daniel G. Amen, MD[1]
Medical Director, Amen Clinics, Inc.

Kristen Willeumier, PhD[1]
Director of Research, Amen Clinics, Inc.

Derek Taylor, BS[1]
Research Associate, Amen Clinics, Inc.

Sandlin Lowe, MD[1]
Psychiatrist, Amen Clinics, Inc.

Cyrus Raji, MD, PhD[2]
Department of Radiology, UCLA Medical Center

[1]Department of Neuroimaging and Clinical Research, Amen Clinics, Inc., 3150 Bristol, Suite 400, Costa Mesa, CA, 92626, USA

[2]Department of Radiology, UCLA Medical Center, Los Angeles, CA, 90095, USA

Acknowledgments:

Author's Access to Data Statement: Daniel G Amen, MD, had full access to all the data in the study and takes responsibility for the integrity of the data and the accuracy of the data analysis.

References:

1. Association AP (2013) Diagnostic and statistical manual of mental disorders (DSM V). Washington, D.C.: American Psychiatric Association.

2. Association AP (2000) Diagnostic and statistical manual of mental disorders (DSM-IV-TR). 4th (text rev.) ed. Washington, DC: American Psychiatric Association.

3. Goldani AA, Downs SR, Widjaja F, Lawton B, Hendren RL (2014) Biomarkers in autism. Front Psychiatry 5: 100.

4. Connolly JJ, Hakonarson H (2014) Etiology of autism spectrum disorder: a genomics perspective. Curr Psychiatry Rep 16: 501.

5. Liu X, Takumi T (2014) Genomic and genetic aspects of autism spectrum disorder. Biochem Biophys Res Commun 452: 244-253.

6. Persico AM, Napolioni V (2013) Autism genetics. Behav Brain Res 251: 95-112.

7. Miyake K, Hirasawa T, Koide T, Kubota T (2012) Epigenetics in autism and other neurodevelopmental diseases. Adv Exp Med Biol 724: 91-98.

8. Ashwood P, Krakowiak P, Hertz-Picciotto I, Hansen R, Pessah I, et al. (2011) Elevated plasma cytokines in autism spectrum disorders provide evidence of immune dysfunction and are associated with impaired behavioral outcome. Brain Behav Immun 25: 40-45.

9. Masi A, Quintana DS, Glozier N, Lloyd AR, Hickie IB, et al. (2014) Cytokine aberrations in autism spectrum disorder: a systematic review and meta-analysis. Mol Psychiatry.

10. Rossignol DA, Genuis SJ, Frye RE (2014) Environmental toxicants and autism spectrum disorders: a systematic review. Transl Psychiatry 4: e360.

11. Libbey JE, Sweeten TL, McMahon WM, Fujinami RS (2005) Autistic disorder and viral infections. J Neurovirol 11: 1-10.

12. Brown AS (2012) Epidemiologic studies of exposure to prenatal infection and risk of schizophrenia and autism. Dev Neurobiol 72: 1272-1276.

13. Simonoff E, Pickles A, Charman T, Chandler S, Loucas T, et al. (2008) Psychiatric disorders in children with autism spectrum disorders: prevalence, comorbidity, and associated factors in a population-derived sample. J Am Acad Child Adolesc Psychiatry 47: 921-929.

14. Silver WG, Rapin I (2012) Neurobiological basis of autism. Pediatr Clin North Am 59: 45-61, x.

15. Centers for Disease Control and Prevention (2014) Prevalence of Autism Spectrum Disorder Among Children Aged 8 Years — Autism and Developmental Disabilities Monitoring Network, 11 Sites, United States, 2010. Morbidity and Mortality Weekly Report.

16. Rogers SJ, Vismara L, Wagner AL, McCormick C, Young G, et al. (2014) Autism Treatment in the First Year of Life: A Pilot Study of Infant Start, a Parent-Implemented Intervention for Symptomatic Infants. J Autism Dev Disord.

17. Bradshaw J, Steiner AM, Gengoux G, Koegel LK (2014) Feasibility and Effectiveness of Very Early Intervention for Infants At-Risk for Autism Spectrum Disorder: A Systematic Review. J Autism Dev Disord.

18. Orinstein AJ, Helt M, Troyb E, Tyson KE, Barton ML, et al. (2014) Intervention for optimal outcome in children and adolescents with a history of autism. J Dev Behav Pediatr 35: 247-256.

19. Levy SE, Mandell DS, Schultz RT (2009) Autism. Lancet 374: 1627-1638.

20. Anagnostou E, Taylor MJ (2011) Review of neuroimaging in autism spectrum disorders: what have we learned and where we go from here. Mol Autism 2: 4.

21. Amaral DG, Schumann CM, Nordahl CW (2008) Neuroanatomy of autism. Trends Neurosci 31: 137-145.

22. Coghlan S, Horder J, Inkster B, Mendez MA, Murphy DG, et al. (2012) GABA system dysfunction in autism and related disorders: from synapse to symptoms. Neurosci Biobehav Rev 36: 2044-2055.

23. Just MA, Keller TA, Malave VL, Kana RK, Varma S (2012) Autism as a neural systems disorder: a theory of frontal-posterior underconnectivity. Neurosci Biobehav Rev 36: 1292-1313.

24. Travers BG, Adluru N, Ennis C, Tromp do PM, Destiche D, et al. (2012) Diffusion tensor imaging in autism spectrum disorder: a review. Autism Res 5: 289-313.

25. Stanfield AC, McIntosh AM, Spencer MD, Philip R, Gaur S, et al. (2008) Towards a neuroanatomy of autism: a systematic review and meta-analysis of structural magnetic resonance imaging studies. Eur Psychiatry 23: 289-299.

26. Courchesne E, Yeung-Courchesne R, Press GA, Hesselink JR, Jernigan TL (1988) Hypoplasia of cerebellar vermal lobules VI and VII in autism. N Engl J Med 318: 1349-1354.

27. Hollander E, Anagnostou E, Chaplin W, Esposito K, Haznedar MM, et al. (2005) Striatal volume on magnetic resonance imaging and repetitive behaviors in autism. Biol Psychiatry 58: 226-232.

28. Sears LL, Vest C, Mohamed S, Bailey J, Ranson BJ, et al. (1999) An MRI study of the basal ganglia in autism. Prog Neuropsychopharmacol Biol Psychiatry 23: 613-624.

29. Haznedar MM, Buchsbaum MS, Hazlett EA, LiCalzi EM, Cartwright C, et al. (2006) Volumetric analysis and three-dimensional glucose metabolic mapping of the striatum and thalamus in patients with autism spectrum disorders. Am J Psychiatry 163: 1252-1263.

30. Herbert MR, Ziegler DA, Makris N, Filipek PA, Kemper TL, et al. (2004) Localization of white matter volume increase in autism and developmental language disorder. Ann Neurol 55: 530-540.

31. Kwon H, Ow AW, Pedatella KE, Lotspeich LJ, Reiss AL (2004) Voxel-based morphometry elucidates structural neuroanatomy of high-functioning autism and Asperger syndrome. Dev Med Child Neurol 46: 760-764.

32. Rojas DC, Camou SL, Reite ML, Rogers SJ (2005) Planum temporale volume in children and adolescents with autism. J Autism Dev Disord 35: 479-486.

33. Courchesne E, Press GA, Yeung-Courchesne R (1993) Parietal lobe abnormalities detected with MR in patients with infantile autism. AJR Am J Roentgenol 160: 387-393.

34. Via E, Radua J, Cardoner N, Happe F, Mataix-Cols D (2011) Meta-analysis of gray matter abnormalities in autism spectrum disorder: should Asperger disorder be subsumed under a broader umbrella of autistic spectrum disorder? Arch Gen Psychiatry 68: 409-418.

35. Philip RC, Dauvermann MR, Whalley HC, Baynham K, Lawrie SM, et al. (2012) A systematic review and meta-analysis of the fMRI investigation of autism spectrum disorders. Neurosci Biobehav Rev 36: 901-942.

36. Yang WH, Jing J, Xiu LJ, Cheng MH, Wang X, et al. (2011) Regional cerebral blood flow in children with autism spectrum disorders: a quantitative (9)(9)mTc-ECD brain SPECT study with statistical parametric mapping evaluation. Chin Med J (Engl) 124: 1362-1366.

37. Wilcox J, Tsuang MT, Ledger E, Algeo J, Schnurr T (2002) Brain perfusion in autism varies with age. Neuropsychobiology 46: 13-16.

38. Carina Gillberg I, Bjure J, Uvebrant P, Vestergren E, Gillberg C (1993) SPECT (Single Photon Emission Computed Tomography) in 31 children and adolescents with autism and autistic-like conditions. Eur Child Adolesc Psychiatry 2: 50-59.

39. Kaya M, Karasalihoglu S, Ustun F, Gultekin A, Cermik TF, et al. (2002) The relationship between 99mTc-HMPAO brain SPECT and the scores of real life rating scale in autistic children. Brain Dev 24: 77-81.

40. Ito H, Mori K, Hashimoto T, Miyazaki M, Hori A, et al. (2005) Findings of brain 99mTc-ECD SPECT in high-functioning autism--3-dimensional stereotactic ROI template analysis of brain SPECT. J Med Invest 52: 49-56.

41. Sasaki M, Nakagawa E, Sugai K, Shimizu Y, Hattori A, et al. (2010) Brain perfusion SPECT and EEG findings in children with autism spectrum disorders and medically intractable epilepsy. Brain Dev 32: 776-782.

42. Amen DG, Hanks C, Prunella J (2008) Predicting positive and negative treatment responses to stimulants with brain SPECT imaging. J Psychoactive Drugs 40: 131-138.

43. Amen DG, Hanks C, Prunella J (2008) Preliminary evidence differentiating ADHD using brain SPECT imaging in older patients. J Psychoactive Drugs 40: 139-146.

44. Chang W, Henkin RE, Buddemeyer E (1984) The sources of overestimation in the quantification by SPECT of uptakes in a myocardial phantom: concise communication. J Nucl Med 25: 788-791.

45. Pluim JP, Maintz JB, Viergever MA (2003) Mutual-information-based registration of medical images: a survey. IEEE Trans Med Imaging 22: 986-1004.

46. Ibáñez L, Schroeder W, Ng L, Cates J, Consortium t, et al. (2003) The ITK Software Guide. Kitware, Inc.

47. Tzourio-Mazoyer N, Landeau B, Papathanassiou D, Crivello F, Etard O, et al. (2002) Automated anatomical labeling of activations in SPM using a macroscopic anatomical parcellation of the MNI MRI single-subject brain. Neuroimage 15: 273-289.

48. Thomas J, Tilanus CB (1964) A note on the estimation of the location parameters of the Cauchy distribution. Journal of the American Statistical Association 61: 852-855.

49. Mai JK, Paxino G, Voss T (1997) Atlas of the Human Brain. San Diego, CA: Academic Press.

50. Trevarthen C, Delafield-Butt JT (2013) Autism as a developmental disorder in intentional movement and affective engagement. Front Integr Neurosci 7: 49.

51. Lombardo MV, Chakrabarti B, Bullmore ET, Consortium MA, Baron-Cohen S (2011) Specialization of right temporo-parietal junction for mentalizing and its relation to social impairments in autism. Neuroimage 56: 1832-1838.

52. Li W, Mai X, Liu C (2014) The default mode network and social understanding of others: what do brain connectivity studies tell us. Front Hum Neurosci 8: 74.

53. Baron-Cohen S, Ring HA, Wheelwright S, Bullmore ET, Brammer MJ, et al. (1999) Social intelligence in the normal and autistic brain: an fMRI study. Eur J Neurosci 11: 1891-1898.

54. Rumsey JM, Ernst M (2000) Functional neuroimaging of autistic disorders. Ment Retard Dev Disabil Res Rev 6: 171-179.

55. Ohnishi T, Matsuda H, Hashimoto T, Kunihiro T, Nishikawa M, et al. (2000) Abnormal regional cerebral blood flow in childhood autism. Brain 123 (Pt 9): 1838-1844.

56. George MS, Costa DC, Kouris K, Ring HA, Ell PJ (1992) Cerebral blood flow abnormalities in adults with infantile autism. J Nerv Ment Dis 180: 413-417.

57. Mountz JM, Tolbert LC, Lill DW, Katholi CR, Liu HG (1995) Functional deficits in autistic disorder: characterization by technetium-99m-HMPAO and SPECT. J Nucl Med 36: 1156-1162.

58. Landrigan PJ (2010) What causes autism? Exploring the environmental contribution. Curr Opin Pediatr 22: 219-225.

59. Ryu YH, Lee JD, Yoon PH, Kim DI, Lee HB, et al. (1999) Perfusion impairments in infantile autism on technetium-99m ethyl cysteinate dimer brain single-photon emission tomography: comparison with findings on magnetic resonance imaging. Eur J Nucl Med 26: 253-259.

Illustrations and Figures:

Figure 1: 3D Surface and Active SPECT Scans

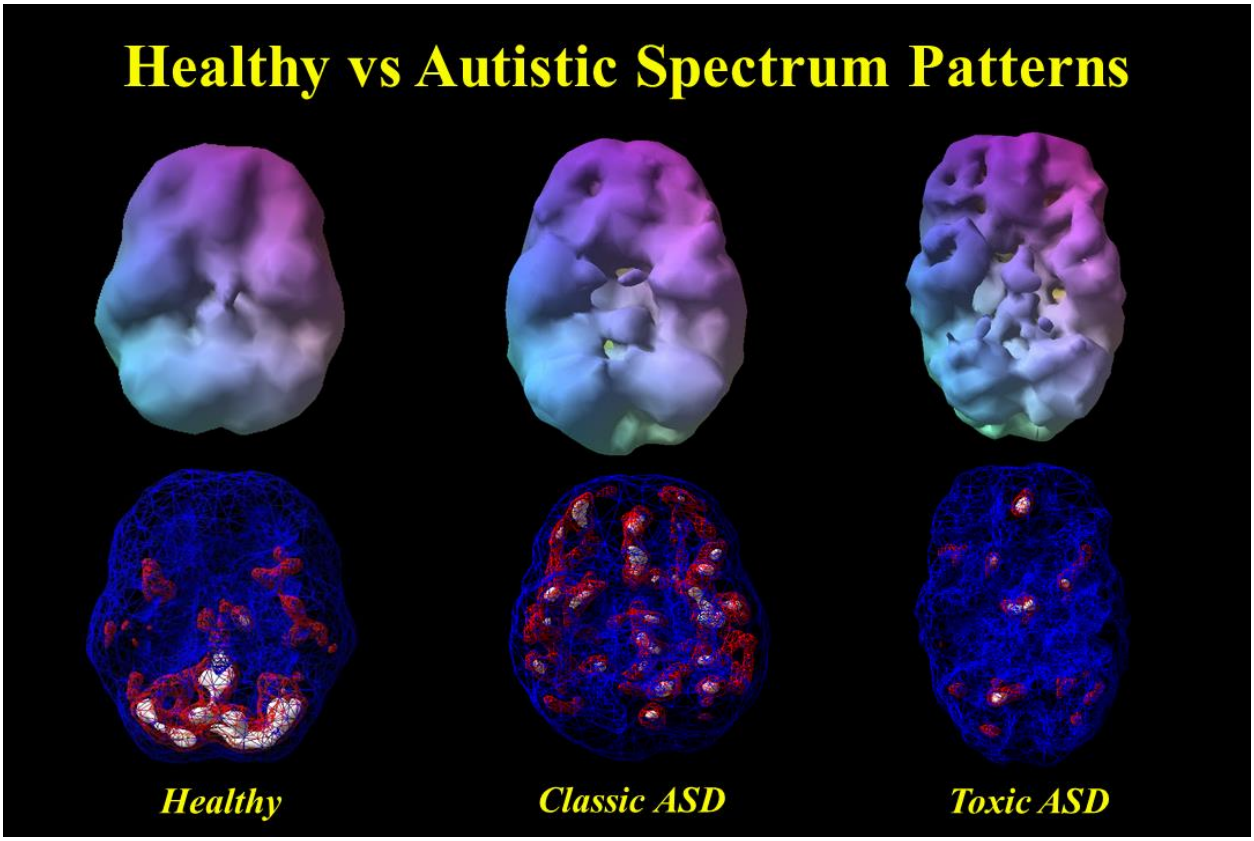

Figure Legend 1: Top row, underneath surface scans, threshold set at 55%, looking at top 45% of brain perfusion. Bottom row, underneath active scans where blue = 55%, looking at top 45% of brain perfusion, red = 85% and white 93%. Healthy shows full even, symmetrical perfusion with most active area in cerebellum. Classic ASD shows decreased cerebellar perfusion, especially in the area of the vermis, looking like an hourglass or free weight pattern. There is also often increased anterior cingulate, medial prefrontal and insular or basal ganglia perfusion. Many patients with ASD do not have

the classic pattern. As shown above a “toxic” pattern with overall decreased perfusion is often seen.

Tables and captions:

Table 1a: Adult Demographics

	ASD Adult	Control Adults	ASD Adults Non-Mood Disorder	Mood disorder Adults	ASD Adults Non-anxiety Disorder	Anxiety disorder Adults	ASD Adults Non-ADHD	ADHD Adults	Healthy Controls
Number of subjects (n)	289	289	115	115	111	111	103	103	99
Males	230	230	96	96	95	95	82	82	42
Females	59	59	19	19	16	16	21	21	56
Age Range	18-67	18-67	18-72	18-76	18-72	18-69	18-67	18-66	18-84
Age	28±11.9	29±11.6	27±11.2	27±11.1	27±11.3	28±10.9	27±10.7	27±11.1	43±-17.1
Brain Trauma	105	105	41	41	40	40	38	38	3
PTSD	18	18	5	5	0	0	2	2	0
Bipolar	11	11	0	15	11	11	5	5	0
Depressed	64	64	0	60	17	17	23	23	0
Anxiety	181	181	62	62	0	111	66	66	0
Schizophrenia /Psychosis	18	3	9	9	7	1	8	8	0
ADHD	184	184	60	60	75	75	0	103	0
Substance abuse	16	16	5	5	8	8	10	10	0

Table 1b: Child Demographics

	ASD	Control	ASD Non-Mood Disorder	Mood Disorder	ASD Non-Anxiety Disorder	Anxiety Disorder	ASD Non-ADHD	ADHD
Number of subjects (n)	644	644	330	330	312	312	154	154
Males	528	527	285	285	265	265	128	128
Females	116	117	45	45	47	47	26	26
Age Range	0-17	1-17	0-17	1-17	1-17	2-17	1-17	3-17
Age	11±-3.5	11±-3.5	10 ±-3.6	11±-3.5	10±-3.6	11±-3.3	11±-3.8	11±-2.9
Brain Trauma	172	171	87	85	81	81	35	34
PTSD	15	15	5	5	0	0	4	4
Bipolar	35	34	1	56	22	22	11	11
Depressed	46	45	1	84	13	13	13	13
Anxiety	339	339	171	171	0	312	74	74
Schizophrenia/ Psychosis	6	1	2	2	1	0	0	0
ADHD	497	497	251	251	233	233	0	154
Substance Abuse	2	2	1	1	1	1	0	0

Table 2: Adults ROC Analysis of Task v Rest Scans
Comparison of Quantitative ROIs with Visual Readings (VR)

Accuracy Sensitivity Specificity CIs/Sig.	ASD (n=289) vs Healthy Controls (n=99)	ASD vs Mood Disorders* (n=115)	ASD (n=127) vs Anxiety Disorders** (n=111)	ASD vs ADHD (n=103)	ASD vs Matched Non-ASD Controls (n=289)
Acc REST ROI	100 (1-1/.00)	100 (1-1/.00)	100 (1-1/.00)	100 (1-1/.00)	84 (.81-.87/.00)
Acc TASK ROI	100 (1-1/.00)	100 (1-1/.00)	100 (1-1/.00)	100 (1-1/.00)	86 (.83-.89/.00)
Sens REST ROI	100	100	100	100	79
Sens TASK ROI	100	100	100	100	79
Spec REST ROI	100	100	100	100	74
Spec TASK ROI	100	100	100	100	74
Acc REST VR	98 (.96-.99/.00)	89 (.84-.93/.00)	93 (.90-.97/.00)	89 (.85-.93/.00)	73 (.69-.78/.00)
Acc TASK VR	96 (.94-.98/.00)	92 (.88-.96/.00)	88 (.84-.93/.00)	93 (.89-.96/.00)	77 (.72-.81/.00)
Sens REST VR	90	80	88	85	68
Sens TASK VR	93	85	82	86	70
Spec REST VR	90	79	85	79	67
Spec TASK VR	90	80	80	85	70

*Mood Disorders include major depression, dysthymia, bipolar disorder, cyclothymia and depressive disorder NOS
**Anxiety Disorders include generalized anxiety disorder, panic disorder, posttraumatic stress disorder, simple and social phobias, and obsessive compulsive disorder

Acc: Accuracy, Sens: Sensitivity, Spec: Specifity

Table 3: Children ROC Analysis of Task v Rest Scans
Comparison of Quantitative ROIs with Visual Readings (VR)

Accuracy Sensitivity Specificity CIs/Sig.	ASD vs Mood Disorders* (n=330)	ASD vs Anxiety Disorders** (n=312)	ASD vs ADHD (n=154)	ASD vs Matched Non-ASD controls (n=644)
Acc REST ROI	92 (.89-.94/.00)	94 (.92-.96/.00)	96 (.94-.98/.00)	89 (.86-.92/.00)
Acc TASK ROI	93 (.91-.95/.00)	89 (.86-.92/.00)	95 (.92-.97/.00)	90 (.88-.93/.00)
Sens REST ROI	85	89	90	83
Sens TASK ROI	87	81	88	83
Spec REST ROI	83	88	90	80
Spec TASK ROI	85	80	86	80
Acc REST VR	88 (.84-.92/.00)	86 (.81-.90/.00)	88 (.84-.92/.00)	83 (.79-.88/.00)
Acc TASK VR	84 (.80-.88/.00)	87 (.82-.91/.00)	88 (.84-.92/.00)	78 (.72-.83/.00)
Sens REST VR	80	80	80	76
Sens TASK VR	80	80	80	72
Spec REST VR	78	73	76	75
Spec TASK VR	74	77	79	70

CI = 95% confidence interval

*Mood Disorders include major depression, dysthymia, bipolar disorder, cyclothymia and depressive disorder NOS

**Anxiety Disorders include overanxious disorder, panic disorder, posttraumatic stress disorder, simple and social phobias, and obsessive compulsive disorder

Abbreviations: Acc=Accuracy, Sens=Sensitivity, Spec=Specificity

Table 4a. Regions that Differentiate ASD from Co-Morbid Psychiatric Disorders and from Healthy Controls (HC) in Adults at Rest Using Quantitative ROI

Table 4b. Regions that Differentiate ASD from Co-Morbid Psychiatric Disorders and from Healthy Controls (HC) in Adults at Rest Using Visual Readings (VR)

Table 5a. Regions that Differentiate ASD from Co-Morbid Psychiatric Disorders and from Healthy Controls (HC) in Adults during On-Task Using Quantitative ROI

Table 5b. Regions that Differentiate ASD from Co-Morbid Psychiatric Disorders and from Healthy Controls (HC) in Adults during On-Task Using Visual Readings (VR)

Table 6a. Regions that Differentiate ASD from Co-Morbid Psychiatric Disorders in Children at Rest Using Quantitative ROIs

Table 6b. Regions that Differentiate ASD from Co-Morbid Psychiatric Disorders in Children at Rest Using Visual Readings (VR)

Table 7a. Regions that Differentiate ASD from Co-Morbid Psychiatric Disorders in Children during On-Task Using Quantitative ROIs

Table 7b. Regions that Differentiate ASD from Co-Morbid Psychiatric Disorders in Children during On-Task Using Visual Readings (VR)